

Guiding of 35 TW laser pulses in ablative capillary discharge waveguides

C. McGuffey,¹ M. Levin,² T. Matsuoka,¹ V. Chvykov,¹ G. Kalintchenko,¹ P. Rousseau,¹
V. Yanovsky,¹ A. Zigler,² A. Maksimchuk,¹ and K. Krushelnick¹

¹Center for Ultrafast Optical Science, University of Michigan, Ann Arbor, Michigan 48109, USA

²Hebrew University, Jerusalem 91904, Israel

(Received 30 June 2009; accepted 12 October 2009; published online 19 November 2009)

An ablatively driven capillary discharge plasma waveguide has been used to demonstrate guiding of 30 fs, 35 TW laser pulses over distances up to 3 cm with incident intensity in excess of 4×10^{18} W/cm². The plasma density range over which good guiding was observed was $1\text{--}3 \times 10^{18}$ cm⁻³. The quality of the laser spot at the exit mode was observed to be similar to that at the entrance and the transmitted energy was $\sim 25\%$ at input powers of 35 TW. The transmitted laser spectrum typically showed blueshifting due to ionization of carbon and hydrogen atoms in the capillary plasma by the high intensity laser pulse. The low plasma density regime in which these capillaries operate makes these devices attractive for use in single stage electron accelerators to multi-GeV energies driven by petawatt class laser systems. © 2009 American Institute of Physics. [doi:10.1063/1.3257909]

I. INTRODUCTION

In 1979, it was realized by Tajima and Dawson¹ that high intensity laser pulses can efficiently generate relativistic electron plasma waves in their wake as they travel through a low density plasma. Electron plasma waves can be simply thought of as displacements of free electrons which oscillate at the plasma frequency (i.e., $\omega_{pe} = \sqrt{n_e e^2 / \epsilon_0 m_e}$, where n_e is the electron density, e is the electron charge, and m_e is the electron mass) with respect to the neutralizing background of slower moving, positively charged ions. These displacements of electrons within the plasma give rise to accelerating electric fields, which can be much larger than the radio frequency fields used for particle acceleration in conventional technology. By using the light pressure of a focused laser pulse, relativistic waves (i.e., having a phase velocity close to the speed of light) can be generated. The criterion for producing a large amplitude relativistic plasma wakefield is that the pulse duration of the high intensity laser pulse be less than the relativistic plasma wavelength (which is only dependent on plasma density). The waves produced in this way therefore meet the requirements for efficient high gradient acceleration for charged particles.² In this situation an electron can “surf” on the electric field of a plasma wave picking up energy from the wave just as a surfer picks up energy from a water wave in the ocean.

However, one of the obstacles for producing high energy electron beams using a single stage laser wakefield accelerator (LWFA) is the necessity for a long acceleration length. The peak electron energy from LWFA scales as the inverse of the plasma density; however since the accelerating electric fields within the plasma also decrease with decreasing density this means that the acceleration distances required to achieve energies of several GeV need to be many centimeters. In fact the acceleration distance increases like $n_e^{-3/2}$, which is just due to classical “dephasing” considerations. This dephasing length is the distance over which fast electrons outrun the accelerating part of the relativistic plasma

wave generated in these interactions. The acceleration distance in experiments can also be limited due to laser pump depletion as energy is lost in the generation of the large amplitude wakefields in the plasma.²

For efficiently generating a wakefield the spot size of the laser pulse should be about the relativistic plasma wavelength which scales inversely as the plasma density. This means that as the plasma density decreases the natural laser diffraction distance (Rayleigh range) increases much more slowly than the dephasing distance, implying that extending the interaction distance beyond a Rayleigh range is critical for the generation of multi-GeV electron beams. Consequently there have been many previous experiments to demonstrate techniques to guide high intensity lasers in a plasma over distances longer than the diffraction distance.^{3–12}

Perhaps the most technologically straightforward method for creating such a plasma waveguide is the ablative wall capillary discharge,^{5–8} which establishes a guiding structure by ablating and heating material from the inner walls of a plastic capillary via low current discharges of 200–400 A. Plastic (carbon and hydrogen) is used as the material in order to keep the average Z of the plasma as low as possible. These were the first capillary discharge devices to demonstrate guiding and such capillaries are much easier to construct than gas-filled capillaries (which are typically made of sapphire)⁹ and in addition require no extra pumping capacity in the experimental vacuum chamber. The disadvantage of these waveguides is that they typically have a limited lifetime, generally contain higher Z-ions in the plasma, and it is difficult to control the plasma density.

A significant recent result was the demonstration of extended laser acceleration distances using a hydrogen filled capillary discharge plasma waveguide, which was shown in 2006, to be able to generate accelerated electron beams to 1 GeV over a distance of only 3 cm using a laser power of 40 TW.¹⁰ This was the first measurement of laser produced electron beams in the GeV range and demonstrated guiding using a hydrogen filled-capillary waveguide. In another

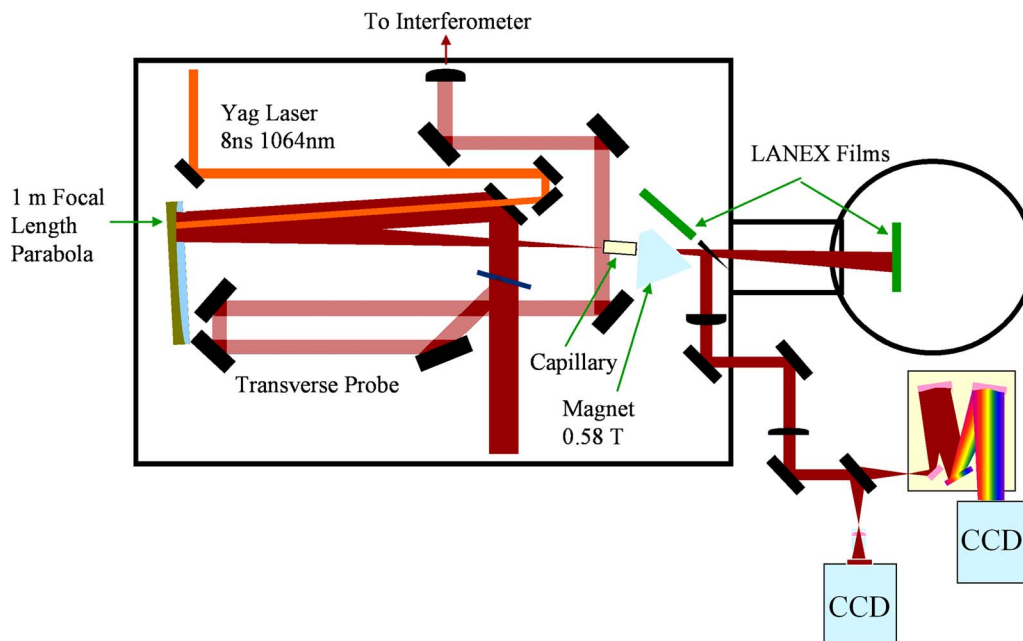


FIG. 1. (Color online) Experimental setup. The igniter pulse and delayed Ti:sapphire pulse are focused by the same parabolic mirror to the entrance of the capillary.

experiment¹¹ a 0.56 GeV electron beam with ~ 10 fC charge was observed using a 4 cm ablative capillary similar to this experiment.

There has subsequently been research to improve the understanding of the details of plasma wave production and electron acceleration in such plasma waveguides, and additional experiments using hydrogen filled capillary waveguides have shown similar acceleration.¹² However another recent experiment showed that the mechanism for generating these beams with hydrogen filled capillaries was more complex than previously thought,¹³ and that electron injection was intimately related to the process of ionization of the target plasma by the intense laser pulse. In such experiments good guiding and an extended propagation distance of the high power laser pulse were a necessary but not sufficient condition for the production of relativistic electron beams from the capillary discharge plasma waveguides. In this work it was found that only when the laser pulse (15 TW) was observed to be ionizing the plasma could accelerated electron beams be measured. Other types of plasma waveguides have also been explored and have been the subject of a significant amount of recent research including the use of gas filled hollow glass capillary waveguides.¹⁴

In this paper we discussed recent experiments undertaken at the University of Michigan in which we demonstrated the successful guiding of laser pulses up to 35 TW through 3 cm using an ablative wall capillary discharge. Although the ablative capillary has some disadvantages as stated above, it also has particular advantages due to its simplicity and the fact that it naturally operates at low plasma density, which is necessary for the acceleration of electron beams beyond several 1 GeV.¹⁵

Although one of the potential disadvantages of ablated wall capillaries for high intensity laser guiding applications is the existence of carbon ions in the plasma when using

polyethylene as the wall material, these ions in the plasma may also play a positive role since the previously mentioned work at higher densities with hydrogen capillaries has found that the higher ionization potential ions may contribute to the efficient injection of electrons into the plasma waves generated during propagation through the plasma waveguide.

In this paper Sec. II will describe the experimental setup, Sec. III will give the experimental results, while Sec. IV will discuss the results and provide interpretation and conclusions.

II. EXPERIMENTAL SETUP

Experiments were performed using the HERCULES Ti:sapphire laser system (35 TW, 30 fs) at the University of Michigan, which was focused by an $f/10$ off-axis parabolic mirror to a $20 \mu\text{m}$ spot diameter [full width at half maximum (FWHM)].¹⁶ 3 cm polyethylene capillaries were used, which had a $400 \mu\text{m}$ diameter bore. The bores were machined from bulk cylindrically shaped polyethylene and initial alignment was done by maximizing the laser light transmitted through the empty capillary at low laser power (<1 mJ per pulse at 10 Hz). Brass electrodes were placed at the ends of the capillary and a capacitor (~ 1 nF) was connected to the electrodes and charged to ~ 20 kV. The discharge was triggered by ablating the inner walls of the capillary with a focused Nd:YAG (yttrium aluminum garnet) laser pulse (30–100 mJ, 10 ns, $\sim 5 \times 10^{10}$ W/cm²). This “igniter pulse” controls the timing of the discharge to within about 5 ns accuracy. A delay generator was used to control the timing between a clock pulse from the Ti:sapphire system and the Nd:YAG q-switch. The experimental setup is shown in Fig. 1.

At the end of its lifetime, a capillary can be replaced in the same amount and only brief realignment is necessary.

The operational lifetime of a typical capillary is several hundred shots. Consequently the high laser power used during the experiment typically did not affect the operation of the discharge, since the limitations in the capillary lifetime are caused mainly by material ablating from the walls during the discharge, rather than during the high intensity laser interaction. The bore diameter increases by as much as 50% over this period, indicating that optimum conditions for guiding will shift throughout this time.

An uncoated glass wedge was used to reflect some of the transmitted light, which was then collected by a lens (2 in. diam \times 20 in. fl) and imaged by a second lens (3 in. diam \times 1 m fl) and 10 \times microscope objective onto a 12-bit charge coupled device to monitor the transmitted laser mode. A beam splitter was also used to send some of this light to an optical spectrometer to monitor changes in the transmitted laser spectrum.

III. EXPERIMENTAL RESULTS

Guiding over 3 cm was achieved, first with the regenerative amplifier level of HERCULES (\sim 1 mJ) and also at powers up to 35 TW. Guiding over this length already offers a significant increase over the self-guided interaction lengths achieved in gas jet targets. As the power levels were increased good guiding conditions were found to be more difficult to obtain, which may have been a result of field ionization and subsequent ionization-induced laser defocusing as well as propagation instabilities (filamentation).

Laser-induced spectroscopy was used to confirm that these ablative capillaries show a parabolic density structure [Fig. 2(a)]. Typical densities of 1 to 3×10^{18} cm $^{-3}$ on axis were achieved with the density increasing with the applied voltage and decreasing at later time. Note that such densities are considerably lower than the densities attainable using gas-filled capillaries.

However, this measurement was taken without a high intensity interaction pulse. To model its propagation through the plasma channel, the plasma refraction index $\eta(r)$, derived from the experimentally measured radial density profile *and* modified via relativistic electron mass increase, was substituted into the envelope equation¹⁷

$$\frac{\partial^2 r_s}{\partial z^2} = \frac{\lambda^2}{\pi^2 r_s^3} + \frac{2}{r_s} \left\langle r \frac{\partial}{\partial r} \eta(r) \right\rangle_r, \quad (1)$$

where the angular brackets denote the intensity-weighted radial average of the quantity enclosed therein. Equation (1) describes the longitudinal evolution of the guided spot radius r_s and can be made formally identical to the equation of motion of a particle subjected to a one-dimensional potential field V_s ,¹⁸ so that $\partial^2 r_s / \partial z^2 = -\partial V_s / \partial r_s$. The function V_s is obtained by integrating the right-hand side of Eq. (1) with respect to r_s and can be called the “guiding potential.” Clearly, the condition $\partial V_s / \partial r_s = 0$ corresponds to a constant (“matched”) spot radius. It can be shown that for a Gaussian beam profile the guiding potential is given by

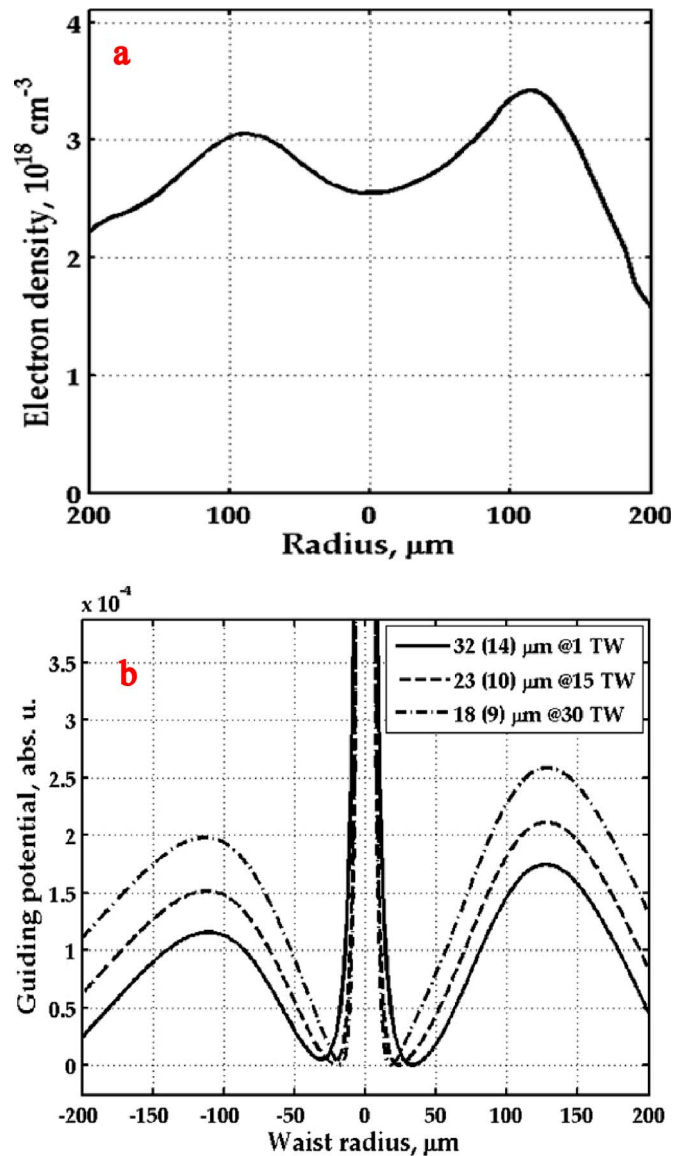


FIG. 2. (Color online) (a) Typical radial density profile for a 3 cm long, 400 μm diameter polyethylene capillary before the arrival of the high intensity pulse. (b) Guiding potentials derived from the profile shown in (a) for three values of the guided beam power. Matched (minimal) guided beam radii are specified for each potential.

$$V_s = - \left[\frac{\lambda^2}{2\pi^2} \frac{1}{r_s^2} + 8 \int_{r_s} \frac{dr_s}{r_s^3} \int_0^\infty r^2 \exp(-2r^2/r_s^2) \frac{\partial \eta}{\partial r} dr \right]. \quad (2)$$

The result of application of Eq. (2) to the radial density profile shown in Fig. 2(a) is presented in Fig. 2(b) for three values of the guided beam power. It can be seen that the matched beam radius decreases as the laser power increases due to relativistic self-focusing. In fact, guiding potential is much more informative than the density profile from which it was derived. The whole range of possibly guided beam radii for a given power can be inferred at a glance.

The timing window appropriate for guiding is determined by the hydrodynamic evolution of the plasma within the capillary. As shown in Fig. 3, the timing window is approximately 150 ns wide. The optimum delay (arrival time of

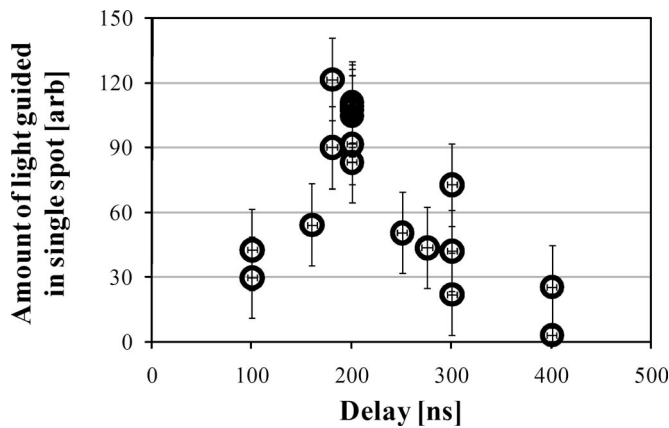


FIG. 3. Timing window over which good guiding (high signal integrated within a $55\ \mu\text{m}$ radius of the peak) is achievable. Laser power is accounted for. Delay is defined as timing between arrival of the igniter and high intensity pulses at the capillary entrance. The discharge is triggered by the igniter pulse. All single shots are from a single experiment at 8 TW, which were known to be at optimal alignment and discharge parameters. Timing jitter was 5 ns. Vertical error bars enclose one standard deviation of all shots with identical parameters taken over many experimental runs.

the high intensity pulse relative to the igniter or discharge triggering pulse) was found to depend on discharge parameters, laser power, as well as an observed slow variation in the alignment and timing as the accumulated number of discharges with the capillary slowly increased the bore diameter.

The images of Fig. 4 demonstrate the observed guiding behavior in these ablated capillary waveguides. A reference shot of the laser at focus is shown (top left). Typical vacuum spot parameters without correction by deformable optics were $20\ \mu\text{m}$ spot diameter with 40% of energy within the FWHM spot. All other images shown in Fig. 4 have the same spatial scale; however, they are imaged 3 cm after laser focus (at the exit of the capillary).

Guided spots contained up to 20% energy within a $35\ \mu\text{m}$ FWHM spot. The total transmitted light is typically 15%–25% of the input. As seen in Fig. 4, many guided spots had fluence within about one order of magnitude of the focused vacuum shot.

The optical spectrum showed a large amount of blueshifted light on most shots when the capillary was discharged. The blueshifted signal as a function of delay (Fig. 5) and lineouts (Fig. 6) at the exit of the capillary show very little blueshifted light for the first ~ 75 ns while the plasma was expanding from the walls. When hydrogen ions and atoms reach the laser axis, weak blueshift of 20–25 nm is observed. This blueshift is nearly constant over the time period of 100–200 ns delay. After ~ 225 ns delay, heavier carbon atoms and ions begin arriving at the laser axis, indicated by a sudden increase in the magnitude of the blueshift, which increases with delay as more carbon ions reach the laser axis. By 400 ns delay, nearly all the light has been blueshifted beyond the blue edge of the initial laser spectrum, followed by a slow decay as recombination takes place at the capillary walls (which we estimate should occur over nanosecond time scales). At low power, ≤ 2 TW, strong blueshift was not observed, and the guiding window was much wider—out to

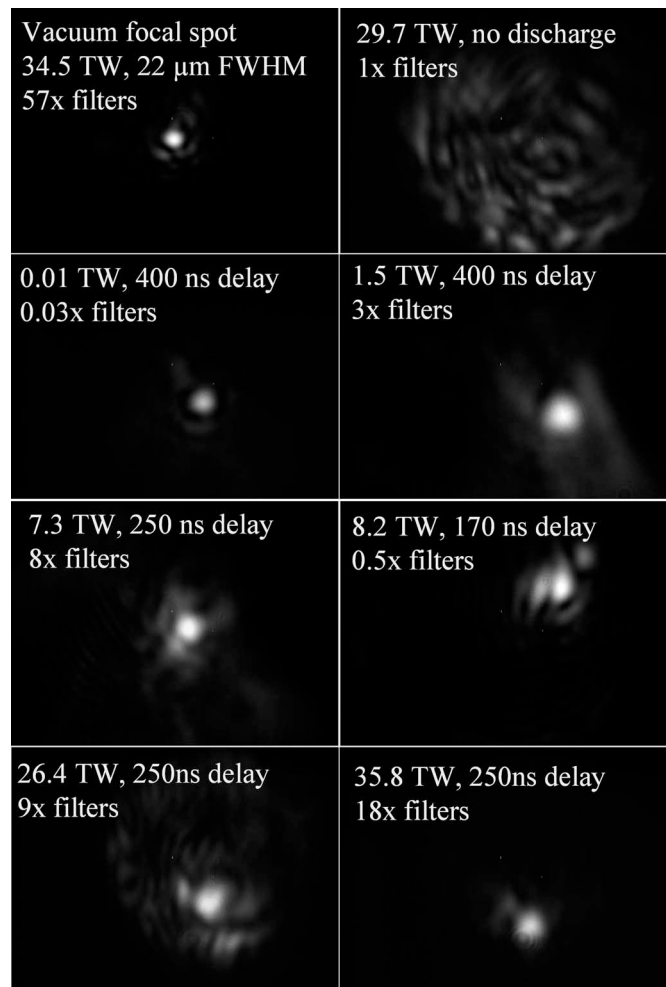


FIG. 4. Top images are reference at focus and capillary rear exit without discharge. Rows two, three, and four show guided laser modes at the capillary exit for various powers. Pointing fluctuation is real.

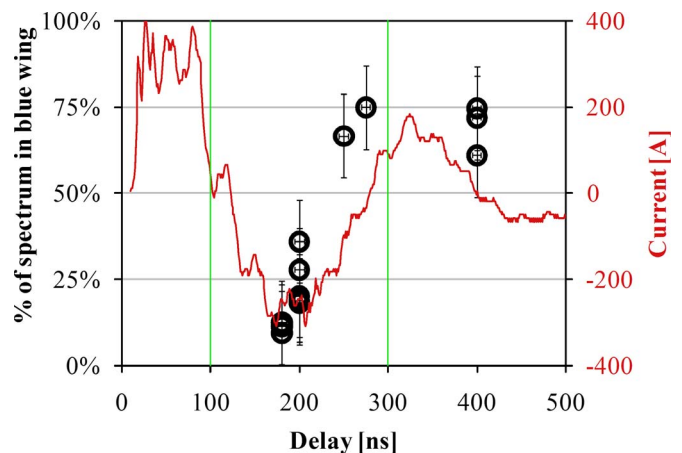


FIG. 5. (Color online) Laser is unaffected until plasma has expanded to fill capillary. Vertical axis is integrated count of laser light, which is higher in frequency than the blue edge of the laser spectrum in vacuum, normalized to the total integrated counts over the entire spectrum. The timing window for guiding is approximately between the green vertical bars. All single shots are from a single experiment at 8 TW. Vertical error bars enclose one standard deviation of all shots with identical parameters taken over many experimental runs. A trace of the discharge current is overlaid.

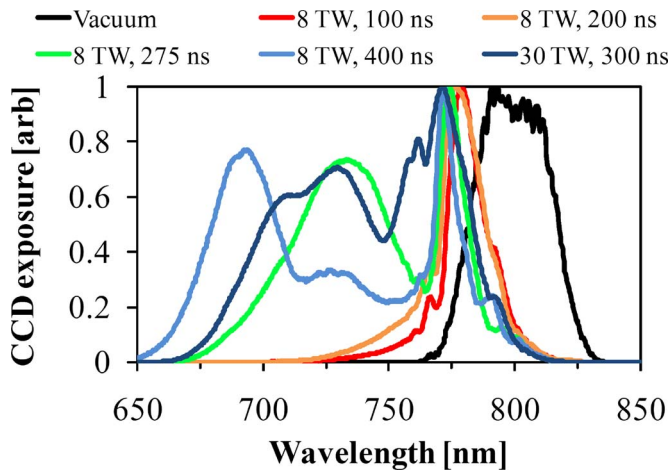


FIG. 6. (Color online) Optical spectra (individually normalized) of transmitted laser light in vacuum and with discharge at various delay and laser power. At short delay, blueshift is weak and insensitive to delay, with the shift of peak increasing slightly with increasing delay. The peaks from the 8 TW shots obey this order. At larger delay, carbon ions from the wall have reached the laser axis, leading to strong ionization blueshift with shift proportional to delay. For higher power, blueshift is more prevalent.

400 ns delay. At high power, ≥ 30 TW, strong blueshift was observed at earlier delay as well as significant spectral broadening and modulation. The guiding window shrank to only include delay of ≤ 250 ns.

This dependence upon laser power suggests that this blueshift is most likely a result of rapid ionization of the gas during the laser pulse,¹⁹ where field ionization causes a change in refractive index which advances at nearly the laser group velocity. The blueshift was much stronger than redshift, as would be expected for a density, which is rapidly increasing in time. This increase is due to field ionization of the low-charge state carbon ions in the polyethylene capillary plasma. The intensity of the triggering Nd:YAG pulse is 10^{10} W/cm², which is too low to ionize hydrogen or carbon atoms, but the flux (~ 500 J/cm²) damages the capillary material. The electrical discharge ensues and any initial ionization is due to this discharge. The discharge has similar parameters to pulsed arc discharge plasmas, which typically have plasma temperatures up to several eV. In the case of our discharge, radiative heat transfer is halted at the walls of the capillary. Consequently plasma at this temperature will have very few ions with charge states above the first ionization stage. In contrast, the arrival of the 35 TW pulse with intensity of $\sim 5 \times 10^{18}$ W/cm² is able to ionize carbon fully and oxygen (if there is any water contamination absorbed in the capillary wall) six times (estimated using the barrier-suppression ionization approximation), causing large amounts of blueshift,

$$\frac{\Delta\lambda}{\lambda^3} = -\frac{L}{2c} \frac{\partial n_e(t)}{\partial t n_c}, \quad (3)$$

where $\Delta\lambda$ is the shift in wavelength, L is the interaction length, n_e is the electron density, and n_c is the critical density. Thus, blueshift is an indication of rapid field ionization, which will be most prevalent on the laser axis where intensity is highest. The overall blueshift will increase linearly

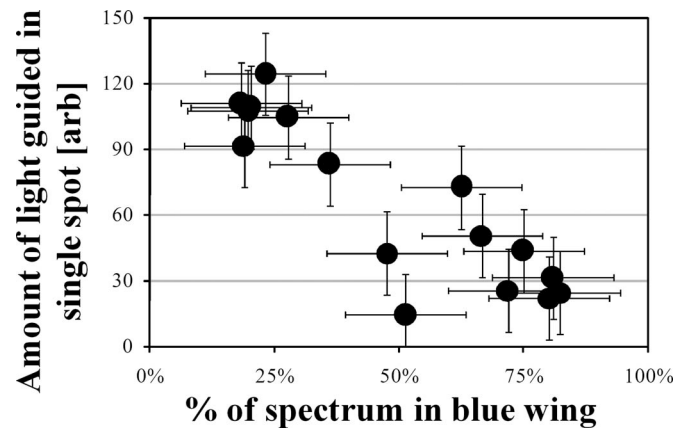


FIG. 7. Quality of guiding is diminished when strong blueshifting is observed. Axes and error bars are the same as in Figs. 3 and 5. All shots are from a single experiment at 8 TW.

with the number of electrons freed by ionization so that full ionization of carbon will result in a six times shift compared with ionization of hydrogen at the same atomic density. In reality, the situation is more complicated than a uniform shift, where considerations must include broadening due to self-phase modulation over the long guided region, spatial extent of the pulse, and interaction of the pulse with the wakefield.^{20–22} Modulation of the spectrum occurs due to interaction of the pulse with wakefield density perturbations and can be substantial for pulses, which are much longer than the plasma wavelength. For our short pulse case, however, the multiple spectral peaks may be due to different ionization states being reached at different spatial regions around the pulse. Indeed, by inspection of the spectra, the blueshifted peak has the greatest shift on axis and lesser shift in the spatial wings (curves in Fig. 6 are integrated in the spatial axis). A redshift shoulder is also observed in some shots, but at two orders of magnitude lower intensity. The dominance of blueshift over redshift suggests our shift is due to ionization rather than pulse/wakefield interaction. Because refractive guiding requires a minimum density on axis, strong field ionization on axis can degrade or even prevent guiding. The parabolic densities measured by laser-induced spectroscopy do not take this into account, as no high intensity pulse was present. This may account for the increased difficulty of achieving guiding at higher powers. As shown in Fig. 7, shots that were best guided were those that had the least amount of blueshifted light.

This indicates that in addition to proper alignment of the capillary and appropriate timing of the discharge, field ionization plays an important role in the quality of guiding. There exists a limit on the intensity which can be guided through the discharge on hand. In other words, a pulse of certain energy should not be focused below a waist radius at which the intensity is enough for the ionization to be significant throughout the capillary length.

In these experiments no accelerated electrons were observed from the interaction of the laser pulse with the waveguide plasma at 35 TW, although electrons were observed in Ref. 11. This is likely due to the density being below that required for wave breaking and self-injection at this power

(Ref. 11 used 3.8 J whereas we define 35 TW as 1.67 J total on target in 30 fs). Alternatively, electrons may be produced but with charge less than our detection level. Reference 11 reports charge of approximately tens of femtocoulomb per shot, whereas our detection limit is estimated at 300 fC.

IV. DISCUSSION

The quality of guiding at 35 TW was observed to be good. Parameters of the guided spot suggest that after 3 cm of propagation, the laser intensity drops only by an order of magnitude (although the transmitted pulse duration is unknown). If carbon is fully ionized by the 35 TW pulse as predicted by barrier suppression ionization, the effects of field ionization may be no worse at several hundred terawatts. Additionally, self-focusing may contribute to self-propagation more at higher powers.

While it is clear that field ionization is correlated with degradation of the observed guiding, the presence or absence of blueshift can be unpredictable. Strong blueshift is occasionally observed at earlier delay than anticipated, especially at high power, and reproducibility of guiding is $\sim 50\%$ even when all discharge parameters are optimized. This is most likely due to laser pointing fluctuations of up to 30 μrad and/or laser energy shot-to-shot fluctuation of up to $\pm 10\%$. Laser energy fluctuations will affect the strength of ionization blueshift. A 30 μm radial shift in the laser focal position is a significant fraction of the size of the guiding channel, as seen in Fig. 2, which could explain the low reproducibility of guiding. Guiding was observed to be sensitive to alignment of the capillary within 20 μm . Pointing fluctuation will also affect the delay at which the laser focus comes into contact with carbon ions, causing ionization blueshift.

While using this low-charge-state ablative plasma adds an additional complication compared with hydrogen-filled capillaries, it may also allow for a simple down-ramp accelerator.²³ At the front of the capillary, field ionization will create a high electron density plasma, allowing electron injection, and as the laser is depleted fewer charge states will be field ionized. This is not the case for hydrogen-filled capillaries, which are nearly fully ionized upon arrival of the laser pulse. Both capillary designs allow control of the density within the capillary, but control is typically more straightforward using hydrogen-filled capillaries by merely changing the neutral gas pressure. Hydrogen-filled capillaries also offer longer lifetime; however “revolver” style ablative capillaries with many bores in a single bulk cylinder may increase the time between capillary replacements. Such capillaries have been manufactured. Lifetime may also increase significantly if every shot is well guided. The effects of ionization blueshift are believed to have been observed in gas-filled capillaries as well¹³ with similar dependence on delay. In this case the amount of ablated wall material is presumably much smaller than in ablative capillaries, and ionization blueshift does not seem to be detrimental to guiding. It is believed that barrier suppression ionization of higher charge states may even be beneficial in the process of self-trapping in laser wakefields²⁴ so long as ionization defocusing does not dominate. This suggests that gas-filled capillaries may be

able to increase the trapped charge in capillary wakefield accelerators by using somewhat softer walls.

On shots up to 35 TW, electrons were not observed, i.e., there was no wave breaking or self-trapping. For the density estimate of $1\text{--}3 \times 10^{18} \text{ cm}^{-3}$ this is to be expected. In typical gas jet runs on HERCULES with 35 TW, the required threshold density for self-trapping of detectable electrons is $\sim 9 \times 10^{18}$ (peak density, no axial averaging).²⁵ Increasing laser power to 300 TW will decrease this threshold to $\sim 2 \times 10^{18}$ based on past scaling on HERCULES. To surpass this density within the capillary, the energy of the Nd:YAG laser used to trigger the discharge may be increased (at the cost of decreasing the lifetime of the capillary). Increasing the discharge current may also increase the charge state of the plasma, thus increasing density, but may also decrease the lifetime of the capillary. Using a smaller bore capillary will also increase density. Smaller bore capillaries ($\leq 250 \mu\text{m}$) in conjunction with control of the spot size using adaptive optics will allow use of the appropriate density for injection while remaining close to the matched spot size.

ACKNOWLEDGMENTS

This research was funded by the National Science Foundation (Grant No. PHY-0114336).

- ¹T. Tajima and J. M. Dawson, *Phys. Rev. Lett.* **43**, 267 (1979).
- ²E. Esarey, P. Sprangle, J. Krall, and A. Ting, *IEEE Trans. Plasma Sci.* **24**, 252 (1996).
- ³C. G. Durfee and H. M. Milchberg, *Phys. Rev. Lett.* **71**, 2409 (1993).
- ⁴K. Krushelnick, A. Ting, C. I. Moore, H. R. Burris, E. Esarey, P. Sprangle, and M. Baine, *Phys. Rev. Lett.* **78**, 4047 (1997).
- ⁵Y. Ehrlich, C. Cohen, and A. Zigler, *Phys. Rev. Lett.* **77**, 4186 (1996).
- ⁶B. Greenberg, M. Levin, A. Pukhov, and A. Zigler, *Appl. Phys. Lett.* **83**, 2961 (2003).
- ⁷M. Levin, A. Pukhov, R. F. Hubbard, D. Kaganovich, D. F. Gordon, P. Sprangle, A. Ting, B. Hafizi, and A. Zigler, *Appl. Phys. Lett.* **87**, 261501 (2005).
- ⁸M. Levin, A. Pukhov, A. Zigler, K. Sugiyama, K. Nakajima, R. F. Hubbard, A. Ting, D. F. Gordon, P. Sprangle, and D. Kaganovich, *Phys. Plasmas* **13**, 083108 (2006).
- ⁹A. Butler, D. J. Spence, and S. M. Hooker, *Phys. Rev. Lett.* **89**, 185003 (2002).
- ¹⁰W. P. Leemans, B. Nagler, A. J. Gonsalves, C. Toth, K. Nakamura, C. G. R. Geddes, E. Esarey, C. B. Schroeder, and S. M. Hooker, *Nat. Phys.* **2**, 696 (2006).
- ¹¹T. Kameshima, W. Hong, K. Sugiyama, X. Wen, Y. Wu, C. Tang, Q. Zhu, Y. Gu, B. Zhang, H. Peng, S. Kurokawa, L. Chen, T. Tajima, T. Kumita, and K. Nakajima, *Appl. Phys. Express* **1**, 066001 (2008).
- ¹²S. Karsch, J. Osterhoff, A. Popp, T. P. Rowlands-Rees, Zs. Major, M. Fuchs, B. Marx, R. Hörlein, K. Schmid, L. Veisz, S. Becker, U. Schramm, B. Hidding, G. Pretzler, D. Habs, F. Grüner, F. Krausz, and S. M. Hooker, *New J. Phys.* **9**, 415 (2007).
- ¹³T. P. Rowlands-Rees, C. Kamperidis, S. Kneip, A. J. Gonsalves, S. P. D. Mangles, J. G. Gallacher, E. Brunetti, T. Ibbotson, C. D. Murphy, P. S. Foster, M. J. V. Streeter, F. Budde, P. A. Norreys, D. A. Jaroszynski, K. Krushelnick, Z. Najmudin, and S. M. Hooker, *Phys. Rev. Lett.* **100**, 105005 (2008).
- ¹⁴B. Cros, N. E. Andreev, M. V. Chegotov, P. Mora, and G. Vieux, *Int. J. Mod. Phys. B* **21**, 548 (2007); N. E. Andreev, B. Cros, G. Maynard, P. Mora, and F. Wojda, *IEEE Trans. Plasma Sci.* **36**, 1746 (2008).
- ¹⁵V. Malka, J. Faure, Y. A. Gauduel, E. Lefebvre, A. Rousse, and K. Ta Phuoc, *Nat. Phys.* **4**, 447 (2008); K. Krushelnick, Z. Najmudin, and A. E. Dangor, *Laser Phys. Lett.* **4**, 847 (2007).
- ¹⁶V. Yanovsky, V. Chvykov, G. Kalinchenko, P. Rousseau, T. Planchon, T. Matsuoka, A. Maksimchuk, J. Nees, G. Cheriaux, G. Mourou, and K. Krushelnick, *Opt. Express* **16**, 2109 (2008).

- ¹⁷E. Esarey, P. Sprangle, J. Krall, and A. Ting, *IEEE J. Quantum Electron.* **33**, 1879 (1997).
- ¹⁸M. Liu, H. Guo, B. Zhou, L. Tanga, X. Liua, and Y. Yi, *Phys. Lett. A* **352**, 457 (2006).
- ¹⁹W. M. Wood, G. Focht, and M. C. Downer, *Opt. Lett.* **13**, 984 (1988).
- ²⁰S. C. Wilks, J. M. Dawson, W. B. Mori, T. Katsouleas, and M. E. Jones, *Phys. Rev. Lett.* **62**, 2600 (1989).
- ²¹A. A. Babin, D. V. Kartashov, A. M. Kiselev, V. V. Lozhkarev, A. N. Stepanov, and A. M. Sergeev, *Appl. Phys. B: Lasers Opt.* **75**, 509 (2002).
- ²²C. D. Murphy, R. Trines, J. Vieira, A. J. W. Reitsma, R. Bingham, J. L. Collier, E. J. Divall, P. S. Foster, C. J. Hooker, A. J. Langley, P. A. Norreys, R. A. Fonseca, F. Fiuza, L. O. Silva, J. T. Mendonca, W. B. Mori, J. G. Gallacher, R. Viskup, D. A. Jaroszynski, S. P. D. Mangles, A. G. R. Thomas, K. Krushelnick, and Z. Najmudin, *Phys. Plasmas* **13**, 033108 (2006).
- ²³C. G. R. Geddes, K. Nakamura, G. R. Plateau, C. Toth, E. Cormier-Michel, E. Esarey, C. B. Schroeder, J. R. Cary, and W. P. Leemans, *Phys. Rev. Lett.* **100**, 215004 (2008).
- ²⁴D. Umstadter, J. K. Kim, and E. Dodd, *Phys. Rev. Lett.* **76**, 2073 (1996).
- ²⁵A. Maksimchuk, S. Reed, S. S. Bulanov, V. Chvykov, G. Kalintchenko, T. Matsuoka, C. McGuffey, G. Mourou, N. Naumova, J. Nees, P. Rousseau, V. Yanovsky, K. Krushelnick, N. H. Matlis, S. Kalmykov, G. Shvets, M. C. Downer, C. R. Vane, J. R. Beene, D. Stracener, and D. R. Schultz, *Phys. Plasmas* **15**, 056703 (2008); A. Maksimchuk, S. Reed, N. Naumova, V. Chvykov, B. Hou, G. Kalintchenko, T. Matsuoka, J. Nees, P. Rousseau, G. Mourou, and V. Yanovsky, *Appl. Phys. B: Lasers Opt.* **89**, 201 (2007).